Available online at www.sciencedirect.com
SCIENCE DIRECT®
Journal of Power Sources 136 (2004) 115–121
JOURNAL OF POWER SOURCES
www.elsevier.com/locate/jpowsour

Electrochemical properties of lithium manganese oxides with different surface areas for lithium ion batteries

Koh Takahashi [a], Motoharu Saitoh [a], Norimitsu Asakura [a], Takashi Hibino, Mitsuru Sano [a,*], Miho Fujita [b], Koich Kifune [c]

[a] *Graduate School of Environmental Studies, Nagoya University, Fuiro-cho, Chigusa-ku, Nagoya 464-8601, Japan*
[b] *Graduate School of Natural Sciences, Nagoya City University, Nagoya 467-8501, Japan*
[c] *Faculty of Science, Osaka Women's University, Sakai 590-0035, Japan*

Received 18 February 2004; received in revised form 28 April 2004; accepted 14 May 2004

Available online 2 July 2004

Abstract

Two lithium manganese oxides, $Li_{1.03}Mn_{1.96}O_4$, with different surface areas of 3.55 and 0.68 m^2/g were prepared and their electrochemical properties were studied as positive electrodes for lithium ion batteries. Cycle performance tests gave capacity losses of 9 and 18% at 25 °C, and 28 and 33% at 55 °C for the samples with larger and smaller surface areas, respectively. The recovery of capacity losses have been found on the addition of the conductor after cycles. The defect of the conductivity between the active materials and the conductors was found mostly responsible for the capacity loss in the smaller surface sample at 25 °C. Cycle performance tests in each region of the charge states divided into five regions show that larger capacity losses are observed in rather lower potential states. Storage performances show the largest capacity loss at 10 and 20% of SOC and the less capacity losses at both 0 and 50–100% of SOC in both of the samples. However, in every region, the capacity loss is much smaller in the larger surface sample than in the smaller surface sample. The maximum Mn dissolution is observed to occur at 100% of SOC (4.5 V) and the next is found around 10–20% of SOC in either sample.

Keywords: Lithium manganese oxide; Surface area; Positive electrode property; Lithium ion battery

1. Introduction

Lithium-ion batteries have currently and widely been used in mobile phones because they have advantages over other kinds of batteries; such as high potentials and highly specific energies. Meanwhile, more demands for large-sized lithium-ion batteries have increased for use in electric and hybrid vehicles. However, for such uses, safety, environmental friendliness, and cost performance should be particularly required. In these respects, a spinel-type lithium manganese oxide is considered more proficient than conventionally used $LiCoO_2$ from the points of being safer, richer in natural resources, and more permissible as a positive electrode for an environmental standard.

For the past several years, many studies have been done to develop lithium manganese oxides with less capacity losses at high temperatures [1]. However, a Li ion battery using lithium manganese oxide as a positive electrode has a disadvantage that it deteriorates badly at high temperatures. This has been attributed to the severe capacity loss of a carbon negative electrode on the deposition of Mn ions dissolved out of a lithium manganese oxide [2]. However, a little work on the Mn dissolution in each charged state was found among the published literatures [3–7]. Further research on the Mn dissolution in lithium manganese oxide should lead to better materials as the positive electrode.

As lithium manganese oxides show large potential jumps at the ends of charge and discharge and this can lead to the accurate estimation of their capacities, they are very interesting from the standpoint of capacity loss during cycling as well. Accordingly, they are thought one of the best materials to study mechanism of the capacity loss in batteries. On the contrary, $LiCoO_2$ does not show such a large potential jump at the end of charging, and an accurate measurement of capacities is difficult.

In the present study we characterize electrochemical properties of lithium manganese oxides with different surface areas as the positive electrodes of lithium-ion batteries.

* Corresponding author. Fax: +81 52 789 4808.
E-mail address: sano@info.human.nagoya-u.ac.jp (M. Sano).

0378-7753/$ – see front matter © 2004 Elsevier B.V. All rights reserved.
doi:10.1016/j.jpowsour.2004.05.014

2. Experimental

2.1. Materials

Two lithium manganese oxides were prepared as follows: First 3.6 g of $LiNO_3$ (99%,Wako Pure Chemical Industries, Ltd.) and 29.2 g of $Mn(NO_3)_2{\cdot}6H_2O$ (99%,Wako Pure Chemical Industries, Ltd.) were dissolved together in 10 ml of distilled water. Into the solution was stirred 18 or 54 g of diethyleneglycol (Wako Pure Chemical Industries, Ltd.). Then the mixture was heated at 150 °C to react. The black powders obtained were ground and then calcined in an alumina crucible at 750 °C for 6 h in a conventional electric furnace.

The 1:2 solvent mixture of ethylenecarbonate (EC) to dimethylcarbonate (DMC) with 1 M $LiPF_6$ dissolved was given by Mitsui Chemical (Tokyo, Japan) and contained less than 10 ppm of H_2O. The 2:1 mixture (CB-2) of acetylene black binder to PTFE was available from Soei Tsusho (Osaka, Japan).

2.2. Measurements

Elemental analyses of samples were made with a fluorescent X-ray spectrometric method. The contents of Li and Mn in lithium manganese oxides and of Mn on Li negative electrodes were measured with the conventional method [8] using a Hitachi 180-50 atomic absorption spectrophotometer. Rigaku Rint-2100 X-ray diffractometer monochromated with a graphite crystal was used with Cu Kα radiation to determine the crystal structure. The scanning electron microscopy (SEM) images were taken with a JSM-6301F (JEOL) after samples were covered with vapor-deposited gold film. The specific surface areas of the samples were measured with the conventional BET method using a NOVA-1200 (Quantachrome).

2.3. Electrochemical cells and cycle performance tests

The mixture of 2/3 of the lithium manganese oxide powder and 1/3 of CB-2 was pressed carefully at 200 kg/cm^2 to make it into a disc for the positive electrode of a cell and was then dried at 150 °C for 6 h. Cycle performance tests in charge–discharge were done on a coin-type cell (CR-2032) assembled with Li metal/the electrolyte (EC/DMC = 1/2 with 1 M $LiPF_6$)/the positive electrode and Celgard 2400 as a separator. Charge–discharge curves were recorded galvanostatically with a Nagano BTS-2004 at a current density of 0.5 mA/cm^2. The cut-off potentials for the charge and discharge limits were fixed at 4.3 and 3.5 V (versus Li/Li^+), respectively. All processes of assembling and dismantling the cells were carried out in an argon atmosphere in a glove box (Vacuum Atmosphere Co., CA, USA). Cyclic voltammograms (CVs) were measured with a BAS-100B electrochemical analyzer at a scan rate of 0.1 mV/s. The working electrode was the mixture of 2/3 of the lithium manganese oxide powder and 1/3 of the conductor, CB-2, and both the counter and reference electrodes were lithium foil.

2.4. Addition of the conductor to the positive electrode after cycles

Positive electrodes were taken out of the coin-cells after cycles. The active material was kneaded well with an additional conductor, CB-2. (After this, the final weight ratio of the lithium manganese oxide to CB-2 was about 1:1.) The mixture was pressed at 200 kg/cm^2 to make it into a disc again for a positive electrode and was then dried under vacuum for 3 h. Then each positive electrode pellet was assembled again into a coin-cell similarly as described above and the discharge capacity was measured.[1]

2.5. Cycle performance in each state of charge

The procedure of this part of the experiments is very similar to that described before [6,9]. First, a cell was charged up to 4.5 V and successively discharged down to 3.5 V to evaluate its discharge capacity. Four voltage points between the above high and low cut-off voltages were set at equal intervals where the capacity was divided equally into five regions between 4.5 and 3.5 V. Second, a cell was charged and discharged between a high and a low cut-off voltage in each region, eight times in each region of the above five divisions. In the 11th cycle, it was fully charged to the cut-off voltage (4.5 V) and then discharged to 3.5 V to measure the discharge capacity and such cycles were successively repeated. Thus, in this series of procedures the capacity in each region was measured (see Footnote 1).

2.6. Storage experiment of the lithium manganese oxide as a positive electrode at each constant potential

A cell was charged up to 4.5 V and discharged down to 3.5 V to measure its discharge capacity. It was then charged up again to each voltage with each state of charge: the voltage was 3.5, 3.956, 3.984, 4.003, 4.017, 4.068, 4.117, 4.123, 4.126, 4.139, 4.3, or 4.5 V and 3.5, 3.950, 3.978, 3.999, 4.012, 4.063, 4.114, 4.123, 4.127, 4.135, 4.3, or 4.5 V for the samples prepared with 18 and 54 g diethyleneglycol corresponding to the 0, 10, 20, 30, 40, 50, 60, 70, 80, 90, 98, or 100% of charged state, respectively. Each cell was stored galvanostatically at 55 °C for a week at each constant potential maintained using a Nagano BTS. After the storage, the cell was charged up to 4.5 V and discharged down to 3.5 V to measure its discharge capacity at room temperature. After the storage experiment was finished, each cell was dismantled and a Li negative electrode in the cell was taken out to

[1] The errors of these measurements for discharge capacities are within 0.2 mAh/g and the reproducibility of their runs was fairly good; the errors of the reproducibility are estimated to be about 2–3% for the discharge capacities.

Table 1
Chemical properties of the prepared samples

	Sample 1	Sample 2
Chemical composition	$Li_{1.03}Mn_{1.96}O_4$	$Li_{1.03}Mn_{1.96}O_4$
Lattice constant (Å)	8.232	8.231
Surface area (m^2/g)	3.55	0.68

measure Mn contents on the Li metal. The errors of these measurements for dissolved Mn contents are within 0.01%. The reproducibility of the measurement runs was good; the measurements of Mn quantities are reproduced within errors of 10%.

3. Results and discussion

3.1. Preparation and characterization of lithium manganese oxides with different surface areas

Two lithium manganese oxides were prepared from $LiNO_3$ and $Mn(NO_3)_2$ using different quantities of diethylene glycol as starting materials. We denote the compounds prepared with 18 and 54 g of diethylene glycol as Samples 1 and 2, respectively. Their basic characteristics are summarized in Table 1. Both of the prepared oxides were chemically analyzed and were identified as $Li_{1.03}Mn_{1.96}O$. X-ray diffraction analyses of the samples indicate that their spinel structures and the crystal structures are definitely indexed to a cubic system (the space group Fd3m) with lattice parameters a_0 of 8.232 and 8.231 Å for Samples 1 and 2, respectively.[2] The surface areas of the samples are 3.55 and 0.68 m^2/g for Samples 1 and 2, respectively, as measured with a BET method. Accordingly, both samples have almost the same types of lithium manganese oxides in their compositions and crystal structures, but they have very different surface areas per weight.

Fig. 1 shows SEM images of Samples 1 and 2. In Sample 1 there are a number of primary particles found to have average diameters of 100 nm and secondary particles in diameters of about 1 μm exist as conglomerates of the primary particles. On the other hand, in Sample 2, most of primary particles are larger than 300 nm in diameter and they seem to form well-developed crystal planes. Further, secondary particles in Sample 2 look to aggregate more primary particles than in Sample 1. From these SEM observations, Sample 1 has larger surface areas per weight than Sample 2 and this is consistent with the result of the BET experiment.

Samples 1 and 2 with the same chemical compositions and similar lattice constants but different surface areas per weight were prepared from different quantities of diethylene glycol. But, why the surface area of the samples largely differs between the two has yet remained unexplained. This should be deduced in the future.

[2] The experimental error of the lattice constant is less than 0.001 Å.

To characterize the electrochemical properties of both samples, their CVs were measured at cut-off voltages between 3.5 and 4.3 V, as shown in Fig. 2. The CVs of both samples show two distinct redox peaks at about 4.00 and 4.12 V and are similar to each other. This two-step profile is characteristic of spinel-type lithium manganese oxides. Thus both samples demonstrate similar electrochemical properties.

3.2. Performances of charge–discharge cycles and Mn dissolutions after cycles

Fig. 3 shows the cycle performances of the samples as positive electrodes at 25 and 55 °C. For cycle performances at 55 °C, first the cells were charged and discharged two times at 25 °C and then cycle performance tests continued at 55 °C. At the 70th cycle at 25 °C, discharge capacities were 114 and 103 mAh/g for Samples 1 and 2, respectively, and at this stage capacity losses were 9 and 18%, respectively. On the other hand, at the 70th cycle at 55 °C discharge capacities decreased to 88 from 123 mAh/g for Sample 1 and to 83 from 123 mAh/g for Sample 2, and their corresponding capacity losses were 28 and 33%, respectively. Therefore, Sample 1 with larger surface area is found to perform better as a positive electrode of a cell than Sample 2 at either 25 or 55 °C. Such a tendency is much clearer at 25 °C than at 55 °C.

After the cycle performance tests were finished, the amounts of manganese deposited on the lithium metal negative electrode were measured. These Mn contents are assumed to be equal to the amounts of manganese ions dissolved into the solution out of the positive electrode material. On this assumption, for Sample 1, the amount ratios of dissolved manganese after the cycles were 0.21 and 1.12% by weight at 25 and 55 °C, respectively, while those of dissolved manganese in Sample 2 after the cycles were 0.15 and 0.58% at 25 and 55 °C, respectively. Consequently, manganese contents dissolved from Sample 2 are about 50% smaller than those from Sample 1 at 55 °C.

3.3. The recovery of capacities by the addition of the conductor after the cycles

For more study of the causes of the capacity loss during cycles, each positive electrode was taken out of the cells after the cycles at 25 or 55 °C and each active material was kneaded enough with additional conductive material, CB-2. Then, a positive electrode pellet was assembled again with the above mixture into a cell and its discharge capacity was measured.

The results are illustrated in Fig. 4. The capacities increased to 120 from 114 mAh/g for Sample 1 and to 117 from 103 mAh/g for Sample 2 at 25 °C. At 55 °C, they increased to 111 from 88 mAh/g for Sample 1 and to 109 from 83 mAh/g for Sample 2.

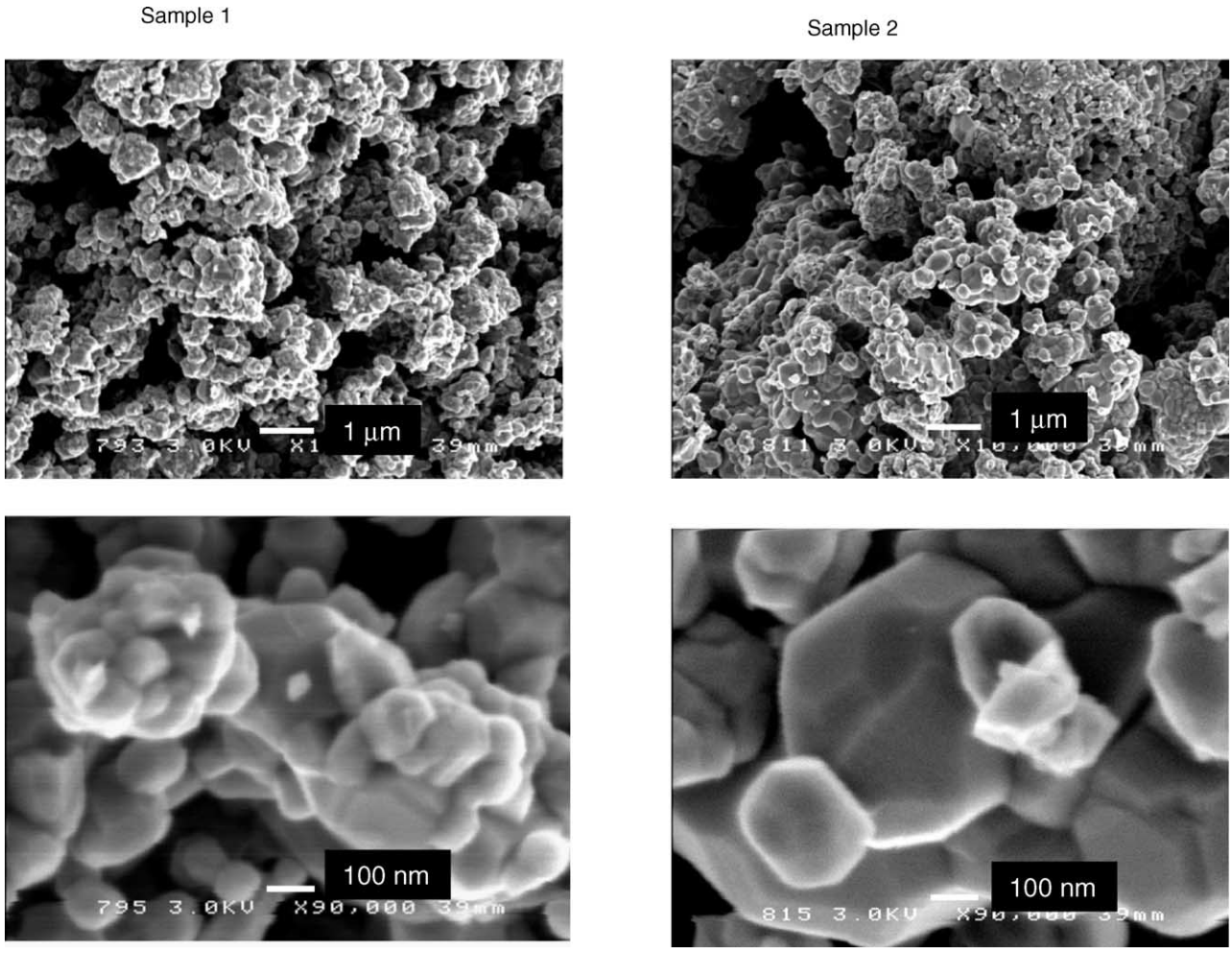

Fig. 1. SEM images of the samples.

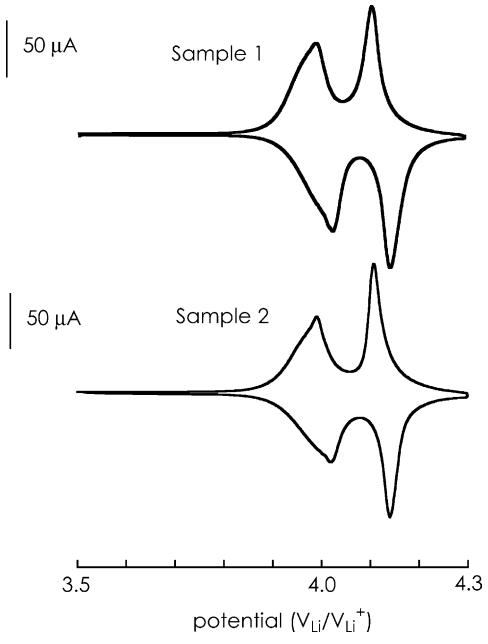

Fig. 2. Cyclic voltammograms of the samples.

In the positive electrode, when ionic or electric conduction is assumed to decrease during cycles, the lost capacity was mostly compensated for and recovered by the addition of conductive material to the active material. The capacity loss remaining after the addition of the conductor is thought to be due to the deterioration of the active material itself. As a result, the capacity loss of a positive electrode during cycles would arise from two key factors: the deterioration of the active material itself and the decrease of the conduction between the active material and the collector.

At 25 °C, the capacity losses derived from the deterioration of the active material itself and the depleted conduction are 5 and 6 mAh/g for Sample 1, respectively, whereas they are 8 and 14 mAh/g for Sample 2. The larger capacity losses due to the conduction depletion is found in Sample 2. As the sample has smaller surface areas, contact areas to the conductor are expected to be smaller. Therefore, close contacts basically tend to be lost and the depletion of conduction could readily occur after all. This will explain why the capacity loss due to the poor conduction is larger than that due to the active material itself in Sample 2. For decreasing the capacity loss, a new binder and/or a new mechanical de-

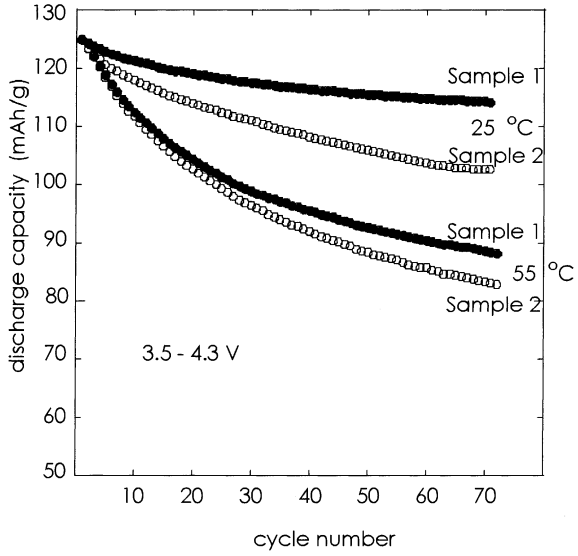

Fig. 3. Cycle performances of the discharge capacities for the samples at 25 and 55 °C.

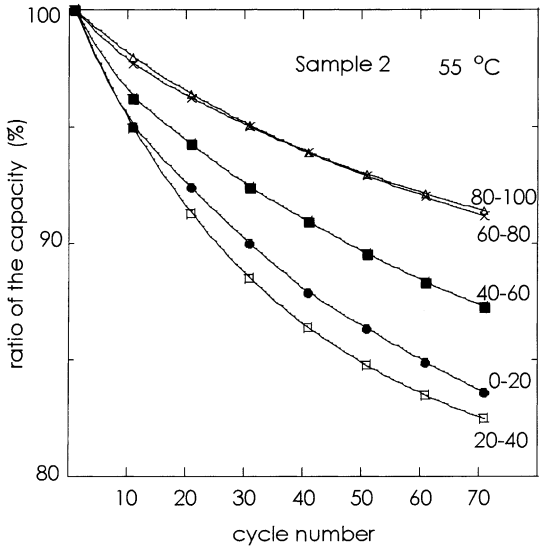

Fig. 5. Cycle performances of discharge capacities at each state of charge in Sample 2 at 55 °C.

vice with a higher ability to keep the close contact between active materials and conductors will be required.

At 55 °C, the capacity losses derived from the deterioration of the active material itself and the depletion of conduction are 12 and 23 mAh/g for Sample 1, and 14 and 26 mAh/g for Sample 2, respectively. The capacity losses due to the poor conduction is about two times larger than those of the active material itself and the depletion of conduction apparently contributes more to the capacity loss in charge–discharge cycles at an elevated temperature.

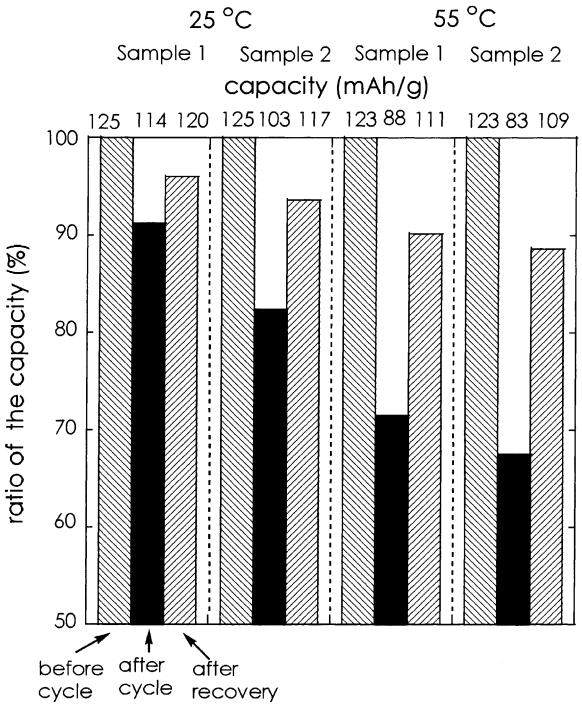

Fig. 4. Recoveries of the capacities with the addition of the conductor to the positive electrode of the samples after cycling at 25 and 55 °C.

3.4. Cycle performance at each state of charge

To specify in what region and how much capacities were lost, cycle performance at each state of charge was examined. The whole range of a discharge capacity was divided into five sections between 3.5 and 4.3 V. Within each of the divisions, a cycle test was carried out to measure the rate of the capacity loss. The experimental details have been described in the previous paper [6] and Footnote 1. Fig. 5 and Table 2 show the results of Sample 2 at 55 °C. Less capacity losses are observed in Sample 1 than in Sample 2 over all sections at both temperatures and this is in accordance with the result of the cycle performance. The orders of good performance for either Sample 1 or 2 at both temperatures are as follows: 80–100% of the state of charge (SOC) > 60–80 > 40–60 > 0–20 > 20. It is particularly noted that larger capacity losses are found at the lower voltage regions. Similar tendencies were also observed in our previous studies [6,8].

3.5. Storage performances at constant potentials

Storage performances and Mn dissolutions in the samples with different surface areas were studied at high temperatures. Fig. 6 shows the results of the measurements. For Sample 2, there is the largest capacity loss at about 10% of SOC and most of the least capacity losses were observed at both 0 and 50–100% region of SOC. Although Sample 1 resembles Sample 2 in the shape of the curve of change, the capacity losses of Sample 1 are less than those of Sample 2 in almost whole regions. The larger capacity loss at 10% of SOC coincides with the worse cycle performance at 0–20 and 20–40% of SOC as described in the previous

Table 2
Cycle performances in each state of charge after 70 cycles at 25 and 55 °C, respectively

State of charge (%)	Ratio of capacity loss (%)			
	Sample 1 (25 °C)	Sample 2 (25 °C)	Sample 1 (55 °C)	Sample 2 (55 °C)
0–20	4.6	6.8	11.8	16.4
20–40	5.4	7.9	13.1	17.5
40–60	3.6	6.1	10.0	12.7
60–80	3.4	4.9	7.0	8.8
80–100	3.0	3.8	6.0	8.6

section. The order of capacity-maintaining ability for both samples in the storage experiments is as follows: 80–100, 60–80 > 40–60 > 0–20, 20–40, and roughly agrees with that of the cycle performance. Thus, the capacity loss in the storage is thought to be closely related with the cycle performance.

Then, let us discuss the relation of the Mn dissolution in the storage with the capacity loss. Amounts of manganese ions dissolved into the solution in Sample 1 are larger than those in Sample 2 as shown in Fig. 6. Maximum Mn dissolution occurs at the highest potential region (4.5 V), that is, at 100% of SOC and the second largest Mn dissolution is seen around 10 and 20% of SOC. The largest capacity losses are observed at 10 and 20% SOC while the smaller capacity loss is found at 100% SOC. Therefore, it seem reasonable to assume that there is not an apparent relationship between the Mn dissolution and the storage performance over all regions except around 10–20% of SOC. The maximum Mn dissolutions at 100% of SOC may be involved in the solvent decomposition at the highest potential state. Thus, getting cut-off voltages lower than 4.5 V will be an efficient mean to suppress the Mn dissolution.

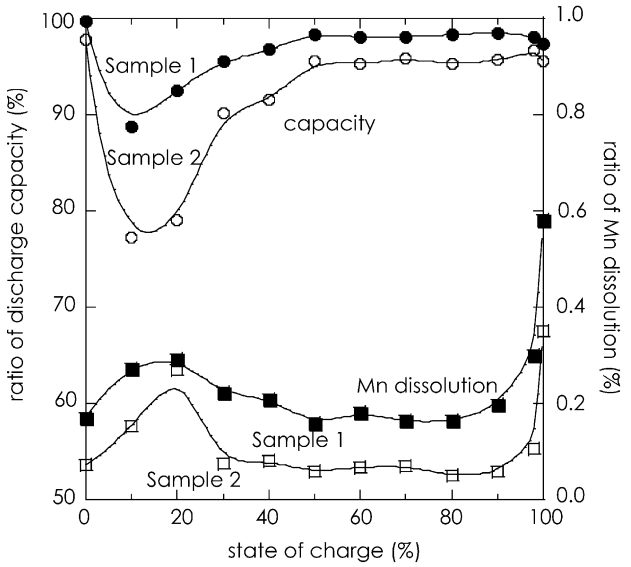

Fig. 6. Storage performances and Mn dissolution of the samples at each constant potential at 55 °C for a week.

4. Conclusions

We prepared two lithium manganese oxides with different surface areas of 3.55 m^2/g (Sample 1) and 0.68 m^2/g (Sample 2) in the same composition of $Li_{1.03}Mn_{1.96}O_4$, with a method using different quantities of diethylene glycol. The cycle performance was found better for Sample 1 (9 and 28% of capacity losses at 25 and 55 °C, respectively) than Sample 2 (18 and 33% of capacity losses at 25 and 55 °C, respectively).

The addition of the conductor gave recoveries of capacities of the positive electrodes after cycles: 120 from 114 mAh/g and 111 from 88 mAh/g at 25 and 55 °C, respectively, for Sample 1, and 117 from 103 mAh/g and 109 from 83 mAh/g at 25 and 55 °C, respectively, for Sample 2. Particularly for the capacity loss of Sample 2 at 25 °C, such lack of conductivity between the active material and the conductor after cycles is considered responsible.

Cycle performance tests in each of five regions of the charge states divided into five regions showed that larger capacity losses were observed in lower potential states. Storage performances at constant potentials showed the largest capacity loss at 10 and 20% of SOC and less capacity losses at both 0 and 50–100% of SOC for both samples.

There was a close relationship found between capacity losses in the storage and those in cycles. Mn dissolution was found to be a maximum at 100% of SOC (4.5 V) and a little less around 10–20% of SOC for both samples. Eventually, no apparent relationship exists between the Mn dissolution and the storage performance at 100% SOC, while such a relationship is apparent around 10–20% SOC.

Acknowledgements

The authors wish to express their sincere thanks to Professor Mitsuo Hoshino of Nagoya University for his kind advice on atomic absorption spectroscopic measurements.

References

[1] Recent papers and references cited herein: R. Premanand, A. Durairajan, B. Haran, R. White, B. Popov, J. Electrochem. Soc. 149 (2002) A54;

K.A. Striebel, E. Sakai, E.J. Cairns, J. Electrochem. Soc. 149 (2002) A61;
M.C. Tucker, J.A. Reimer, E.J. Cairns, J. Electrochem. Soc. 149 (2002) A574;
B.J. Hwang, R. Santhanam, C.P. Huang, Y.W. Tsai, J.F. Lee, J. Electrochem. Soc. 149 (2002) A694.
[2] H. Tsunekawa, S. Tanimoto, R. Marubayashi, M. Fujita, K. Kifune, M. Sano, J. Electrochem. Soc. 149 (2002) A1326.
[3] Y. Xia, M. Yoshio, J. Electrochem. Soc. 144 (1997) 4186.
[4] J.H. Lee, J.K. Hong, D.H. Jang, Y.K. Sun, S.M. Oh, J. Power Sour. 89 (2000) 7.
[5] H. Yamane, T. Inoue, M. Fujita, M. Sano, J. Power Sour. 99 (2001) 60.
[6] H. Yamane, M. Saitoh, M. Sano, M. Fujita, M. Sakata, M. Takada, E. Nishibori, N. Tanaka, J. Electrochem. Soc. 149 (2002) A1514.
[7] M. Saitoh, S. Yoshida, H. Yamane, M. Sano, M. Fujita, K. Kifune, Y. Kubota, J. Power Sour. 122 (2003) 162.
[8] A.M. Bond, D.R. Canterford, Anal. Chem. 43 (1971) 134.
[9] M. Saitoh, M. Sano, M. Fujita, M. Sakata, M. Takata, E. Nishibori, J. Electrochem. Soc. 151 (2004) A17.